CONTRIBUTED POSTER PRESENTATION

1. Cavity Dynamics of Small-Scale Water-Entry

Jeffrey M. Aristoff and John W. M. Bush
Massachusetts Institute of Technology

We present the results of a combined experimental and theoretical investigation of the vertical impact of a hydrophobic sphere with a water surface. Particular attention is given to characterizing the shape of the resulting air cavity in the low Bond number limit. A theoretical model is developed to describe the evolution of the cavity shape, and the pinch-off time is deduced for each of the three experimentally observed cavity types. Theoretical predictions are found to compare favorably with experimental observations.

2. Airflow driven pinch-off of a bubble in a rotating liquid

Raymond Bergmann, Devaraj van der Meer, Anders Andersen, and Tomas Bohr
Technical University of Denmark

3. Particle-Wave Association on a Fluid Interface : Towards a Macroscopic Tunnel Effect ?

Antonin Eddi
Université Paris

A droplet bouncing on a vertically vibrated bath can become coupled to the surface waves it generates. It thus become a "walker" moving at constant velocity on the interface. We showed that the coupling between particule and surface waves can lead to diffraction and interferences patterns. We are now investigating the analogy with quantic tunnel effect in a macroscopic experiment by sending the droplets on an immersed barrier.
Over this barrier, the waves are damped, and we study the ability of the droplet to go across the barrier. The droplet is presenting deterministic or probabilistic behaviours, depending on experimental conditions.

4. Thermal convection with variable transport properties

Francisco Fontenele Araujo
University of Twente

Thermally driven fluid motion usually involves significant variations in transport properties like viscosity and thermal conductivity.
In the context of Rayleigh-B\'enard convection (flow in a container heated from below and cooled from above), such variations can break the top-down symmetries of the velocity, temperature, and density profiles. This symmetry breaking is indicated by the difference $T_{c} - T_{m}$, where T_{c} is the temperature in the center of the convection container and $T_m = (T_{b} + T_{t})/2$ is the mean temperature between the bottom (T_{b}) and top (T_{t}) plates.
On the basis of boundary-layer equations with variable transport properties [1-2], we compute $T_{c} - T_{m}$ as function of $\Delta = T_{b} - T_{t}$. Two different fluids are considered:
gaseous ethane close to its critical point [1] and water [2].
The latter exhibits $T_{c} > T_{m}$ for increasing Δ, meaning that the top boundary-layer becomes thicker than its counterpart at the bottom plate. In contrast, when working fluid is gaseous ethane, the opposite symmetry breaking is observed.
In both cases, our theoretical results are in reasonable agreement with experimental measurements.

References
[1] G. Ahlers, F. Fontenele Araujo, D. Funfschilling, S. Grossmann, and D. Lohse. Physical Review Letters 98, 054501 (2007).
[2] G. Ahlers, E. Brown, F. Fontenele Araujo, D. Funfschilling, S. Grossmann, and D. Lohse. Journal of Fluid Mechanics 569, 409 (2006)

5. Cavity dynamics of a submerging cylinder

Stephan Gekle, Raymond Bergmann, Arjan van der Bos, Devaraj van der Meer, Detlef Lohse
University of Twente

A long, smooth cylinder is dragged through a water surface to create a cavity with an initially cylindrical shape. This surface void then collapses due to the hydrostatic pressure, leading to a rapid and symmetric pinch-off in a single point. Surprisingly, the depth at which this pinch-off takes place does not follow the expected Froude$^{1/3}$ power-law. Instead, it displays three distinct scaling regimes separated by discrete jumps, both in experiment and in numerical simulations (employing a boundary integral code). We quantitatively explain the above behavior by incorporating the influence of the capillary waves which are created as the cylinder passes the water surface into the analysis of the collapse. Our work thus gives further evidence for the non-universality of the void collapse.

6. NUMERICAL ANALYSIS OF FLUID FLOW AND CONCENTRATION DISTRIBUTION OF CHANNELS WITH POROUS LAYER ON THE BASE

Levent DEMİRHAN, Utku GULAN, Hasmet TURKOGLU
Gazi University

In this study, fluid flow and concentration distribution in a parallel-plate channel with a porous layer on the base was numerically analyzed. As it is structurally similar to the flow in the cathode section of the PEM (Polymer Electrolyte Membrane) fuel cell, information has been given both on fuel cell system and the porous materials. Continuity, momentum and concentration equations were discritized by the control volume method and solved using a computer program developed using SIMPLE algorithm. Flows in parallel-plate channel and in a channel whose bottom wall is porous were solved by the software developed in this study. Comparing the results of numerical simulations and the result of analytical solution and results from literature, the mathematical model and program developed were tested. Simulations were made for different values of porosity, Reynolds number and thickness of porous layer. Using the results of these simulations, the effects of these parameters on flow and concentration were analyzed. It was observed that when the porosity of porous layer is increased, the velocity and concentration consumption in this layer also increases. Reducing Reynolds number resulted in increase of dimensionless velocity in this layer and decrease of concentration. As the thickness of the porous layer increases, the dimensionless velocity gradient and concentration decreased. Furthermore, when the porosity of porous layer is increased, the fraction coefficient decreases.

7. Resolution of deterministic lateral displacement devices

Martin Heller
Technical University of Denmark

Particle transport in deterministic lateral displacement devices is governed by convection due to fluid flow and displacement due to interaction with the obstacles in the array [1]. These are deterministic processes and the critical size of particles in these devices is well understood [2]. If deterministic lateral displacement devices are scaled down, diffusion will influence the separation process and affect the critical particle size. We present a simple

iterative model for transport of particles with different sizes in bumper arrays as well as analytical estimates of the critical particle size when diffusion is not negligible.

[1] L. R. Huang, E. C. Cox, R. H. Austin, and J. C. Sturm, Science 304, 987 (2004).
[2] D. W. Inglis, J. A. Davis, R. H. Austin, and J. C. Sturm, Lab Chip 6, 655 (2006).

8. Nonhydrostatic Effects and Stability Properties of Oceanic Flow

Nicole Jeffery
Los Alamos National Laboratory

Stably stratified and rotating flow in the ocean is subject to three types of shear instability: baroclinic, symmetric, and Kelvin-Helmholtz. Stone (1971) hypothesized that the Richardson number (a measure of stratification to shear strength) determines the region of dominance for each instability as well as regions of overlap, and concludes that the hydrostatic baroclinic instability is the most important at the large scales resolved by today's high resolution global ocean models. In this poster, I examine the fully nonhydrostatic inviscid Boussinesq equations with tilted planetary rotation and revisit the stability properties of the baroclinic and symmetric instabilities in Stone's framework. I find an altered picture in which the growth rates of symmetric instabilities shift to larger scales, maximum growth rates for baroclinic instabilities occur at smaller scales, and nonhydrostatic effects play a key role.

9. Polymer Networks as Pressure Sensitive Adhesives – Viscoelastic Guidelines

Mette Krog Jensen
Technical University of Denmark

The present work focuses on the use of polymer networks as pressure sensitive adhesives (PSA). The purpose is to achieve an adhesive which adhere well on a given substrate, while easy to remove without leaving traces. A polymer/crosslinker system with changing degree of cross-linking is used, and Dynamic Mechanical Analysis (DMA) are used to address the fundamental viscoelastic parameters that govern the PSA performance. 90° peel tests are performed, and the measured peel forces are held up against the viscoelastic results. From this comparison basic guidelines for selecting the appropriate polymer/cross-linker system, to achieve the target performance, are given.

10. Sediment transport in a laminar flow

Vincent Langlois
Trinity College Dublin

Transport of sediment by water is involved in many industrial and natural phenomena, and its precise mechanisms remain a major issue. For the bedload transport in particular, several flux laws have been derived from empirical observations or simple mechanical models, but theoretical works on instabilities have showed that these descriptions are not precise enough.
We present here a simple numerical model for the behaviour of a 2D granular bed sheared by a continuous laminar fluid flow. Computation is based on the Molecular Dynamics method, and both the effect of the fluid on the grains, and of the grains on the mean flow are taken into account. Thus the fluid flow automatically adapts to the presence and movements of the grains. We observe that the flux of grains follows Bagnold's power law. The simulations also allow to get access to the detailed characteristics of the grain flow, such as the velocity distribution and the depth of the moving layer.

11.

Erik Martens
Cornell University

12. 3D Modeling of laminar-turbulent transition on wind turbine blades

Gabriel G. Martinez H (Supervisor: Jens Norkær Sørensen)
Technical University of Denmark

Accurate modeling and simulation of the transition process from laminar to turbulent flow is important for a precise design of wind turbine blades. Most of the actual CFD codes assume that the boundary layer is completely turbulent, giving as a result inaccurate prediction of loads and performance.
Depending on the level of turbulence in the incoming flow two different types of scenarios can be found. If the level is relatively low, the flow will pass through linear amplification of the waves, natural transition will occur. If it is higher, non linear behavior will take place immediately and bypass transition will be present. This scenario is the most commonly found.
The laminar/turbulent transition process is related to the stability of the boundary layer, three dimensional and rotational effects; Coriolis and cross flow must be included in the Stability analisys. To study the amplification of the waves hydrodynamic stability approach will be used, a database with the a 3D family of velocity profiles will be used as an input to the Orr-Sommerfeldt (O-S), and, as a result the stability characteristics of all relevant boundary layer shapes will be mapped and stored in an effective database.

13. Micro-size-exclusion chromatography using combined nano- and micro-structuring of polymers

Maria Matschuk, Yanwei Wang, Anders Thomsen, Ole Hassager, Henrik Bruus, Niels B. Larsen
Technical University of Denmark

Fast, efficient, and inexpensive separation of small volumes of macromolecular solutions plays an ever more important role in a number of research fields, e.g. genomics or polymer synthesis. Examples include different sized DNA fragments after cell lysis, or different sized polymers in polymeric solutions: The extraction and amplification of DNA are achieved by well established methods of molecular biology. The yield mostly consists of DNA fragments of slightly different sizes. For the investigation of specific DNA structures it is necessary to separate a fragment of a given size from residual fragments. However, the separation itself of polymer molecules of slightly varying lengths in a given polymeric solution, e.g. after synthesis, is difficult ans relatively expensive due to used chemicals and processes. It therefore becomes an important task to be able to separate and analyze a small amount of a given polymer. Applications relying on separation of macromolecules increasingly make use of lab-on-a-chip systems that ultimately will include all operational steps with very small sample requirements. Therefore, the targeted separation component should allow for integration into such systems. Different separation methodologies may be used, including filtration, sieving, electrophoresis, or chromatography, depending on the properties of the sample. We employ size exclusion chromatography (SEC) to separate macromolecular solutions with particular focus on polymer solutions. SEC is based on the separation of macromolecules by size. Smaller molecules enter a stationary phase (porous matrix) from a mobile carrier phase with higher probability (larger partition coefficient), and hence take longer to exit the separation system than larger particles having a smaller partition coefficient. The application of this principle for a microchip has already been shown for nano-porous alumina [1] using PMMA micro-channels (mobile phase) with a coating of nano-porous alumina membrane (stationary phase). The principle was demonstrated for the separation of DNA fragments with 0.3 kbp and 3.2 kbp, respectively. Another group has shown

the possibilities of nano-structured silicone for the separation of different DNA fragments (2, 5, and 10 kbp) by regular pillar arrays [2].
By using polymer fabrication and processing for combined nano- and microstructuring, we are able to develop the stationary and mobile phase in two steps: (1) the fabrication of structures for the mobile and stationary phase in separate chip parts, and (2) sealing of the microchip. Our micro-size-exclusion chromatography chip (mSECC) is made by injection molding or hot embossing of either polycarbonate or TOPAS (cyclic olefin copolymer). The stationary phase consists of nano-pore arrays of well-defined dimensions, calculated from the size of the macromolecules to be separated. Proof-of-principle chromatograms will result from the optical detection of fluorescently labeled poly(ethylene glycols) separated by the chip system.

[1] T. Sano et. al., "Size-exclusion chromatography using self-organized nanopores in anodic porous alumina", Appl. Phys. Letters, Vol. 83, November 2003
[2] M. Baba, T. Sano, N. Iguchi, K. Iida, T. Sakamoto, and H. Kawaura, "DNA size separation using artificially nanostructured matrix", Appl. Phys. Letters, Vol. 83, August 2003

14. Increasing the accuracy of time resolved PIV measurements

Ulrich Miessner
Delft University of Technology

15. Faraday waves in Bose-Einstein condensates

Alexandru Nicolin
Niels Bohr Institute

Motivated by recent experiments on Faraday waves in Bose-Einstein condensates we investigate both analytically and numerically the dynamics of cigar-shaped Bose-condensed gases subjected to periodic modulation on the transverse confinement. We offer a fully theoretical explanation of the observed parametric resonance, based on a Mathieu-type analysis of the non-polynomial Schrodinger equation. The theoretical prediction for the pattern periodicity versus the driving frequency is directly compared with the experimental data, yielding very good quantitative agreement between the two.

16. Dispersion in microfluidic devices by pressure and electroosmotic driven flow - an experimental and theoretical comperison

V.H.J. Nieborg, R. Lindken, H.J.M. Kramer, G.J. Witkamp, J. Westerweel
University of Technology Delft

In microfluidic systems, dispersion of the sample is an often occurring unwanted effect. Dispersion is an effective increase of a sample its width as a result of a gradient of the velocity profile over the channel width. Dispersion was already investigated by Taylor and Aris in 1954 - 1956, for laminar and turbulent flow. Therefore dispersion is often called Taylor-Aris dispersion. More recently Dutta et al. (2002-2006) has taken a theoretical look at Taylor-Aris dispersion in microfluidic devices with different channel geometries. A different geometry, influences the distribution of the velocity profile over the channel width and therefore influences the Taylor-Aris dispersion directly. In the research performed here we take a look at the Taylor-Aris dispersion in microchannels experimentally as well as theoretically, in the case of pressure driven flow and electroosmotic flow. Very often the dispersion caused by an electroosmotic flow is ignored because there is only a very small velocity distribution over the channel width. However dispersion is still observed and can be quantified. The measurements are done by creating a small tracer plug and

transporting this by pressure and electroosmotic flow and measuring its increase in size. A good agreement between theory and experiments is obtained.

17. Zipping wetting: Filling dynamics during Cassie Baxter to Wenzel transition

Alisia Peters
University of Twente

Many researchers have replicated nature's super-hydrophobic surfaces (like the lotus leaf) with micro-patterns and have described contact angles and contact lines of both the Cassie Baxter and the Wenzel state. The work presented here describes the conditions and kinetics for a transition between these two states. Theoretical calculations, experiments and numerical simulations have provided design criteria based on geometry and material properties. The filling dynamics (speed and pathway) are studied experimentally through a microscope and a high-speed camera and numerically with Lattice Boltzmann simulations. During the transition between the Cassie Baxter state and the Wenzel state (wetting) the kinetics can differ in the x and the y direction. Two speeds are described: the front and zipping speed.

18. In vitro combined measurement of gene expression, shear stress distribution and surface topography of endothelial cells in flow chambers

Massimiliano Rossi
Delft University of Technology

It is postulated that gene expression of endothelial cells is modulated by the shear stress induced by the blood flow in the vessels. We used an optical, non-tactile measurement technique based on micro-PIV to investigate the relationship between shear stress distribution, shape and gene expression on a single-cell level. The cells are cultured in parallel flow chambers and subjected to different flow conditions. The fluid flow velocity in several planes over the cell is measured. From the three-dimensional flow field velocity profiles are extracted and used to reconstruct the cell topography and the shear stress distribution over it. The gene expression measurements are performed with a shear responsive pKLF2-EGFP promoter construct that was transfected in the cells. Results will be shown on human endothelial cells subjected to a constant flow inducing a nominal wall shear stress level of 2.5 Pa.

19. Amplitude equation for under-water sand ripples in one dimension

Teis Schnipper, Keith Mertens, Clive Ellegaard, and Tomas Bohr
Technical University of Denmark and Center for Fluid Dynamics

Sand ripples is a commonly observed structure where sand is exposed to an oscillating flow as created by e.g. surface waves. These structures commonly referred to as vortex ripples have been investigated theoretically and in laboratory experiments for many years starting with the pioneering work by Ayrton and Bagnold. The phenomenology is in many ways similar to classical pattern forming systems like Rayleigh-Bénard convection, but in contrast to the latter, an amplitude equation has never been derived for the periodically driven sand ripples. So far, attempts are based on locally conserving equations.
In this work we present a candidate for an amplitude equation that is neither local or locally conserving. This is justified by experimental observations showing that 1) sand is transported from the bulk to the surface and 2) the separation vortex in the flow creates long-range interaction. The aim is to reproduce one dimensional ripple shapes from a flat bed (primary instability) as well as secondary instabilities i.e. transitions from one rippled pattern to another. Furthermore, we report some new and surprising details about the period doubling bifurcation (doubling the number of ripples) showing long range

interaction. Here, two ripples are initially seen to grow in each trough followed but a collective choice about which one to grow to full size on behalf of the other.

20. Towards an universal criterion of stability for a dry patch in a flowing in film

Julien Sébilleau, J. Sebilleau, L. Lebon and L. Limat
PMMH, ESPCI

Stability of a dry patch in a liquid film flowing down an inclined plate is a subject of industrial interest. In many processes (heat exchangers, coating flows) one needs to avoid their appearance or at least to force their healing. Previous studies [1, 2] propose criterions for the stabilty of dry patchs which are not compatible with experiments. The shape of a dry patch in the Stokes limit [3, 4] is well known but its stability still remains a challenge. In a previous paper,Podgorski *et al* show that the shape results from an equilibrium between capillarity and the weight of the rim and that the radius of curvature at the apex follows :

$$R = m\frac{(1-\cos\theta)^4}{\theta - \sin\theta\cos\theta}\frac{l_c^2 U_c}{\Gamma \sin\alpha}$$

where Γ is the flow rate, α the angle of inclinaison, m a constant taking into account the flow in the rim, U_c the capillary speed and l_c the capillary length. Altought this shape is in excellent agreement with experimental shape of a dry patch, the Podgorski *et al* model does not predict any stability criterion.

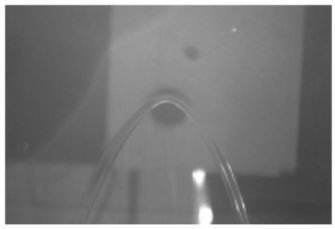

FIG. 1 – Photo of a dry patch in a $\eta = 11,55cP$ oil film

In the present work, we improve the model in the Stokes limit by adding capillary effects due to the radius of curvature at the apex, inertia effects in the rim and hydrostatic pressure effects. This improved model predicts two possible radius of curvature at the apex for the same flow

rate with one of them unstable (see figure2). This allows us to derive a stability criterion for a dry patch in a flowing film in the Stokes limit, which corresponds a critical value for the radius of curvature $R_c \sim 3l_c$ (and also to a critical flow rate Γ_c).

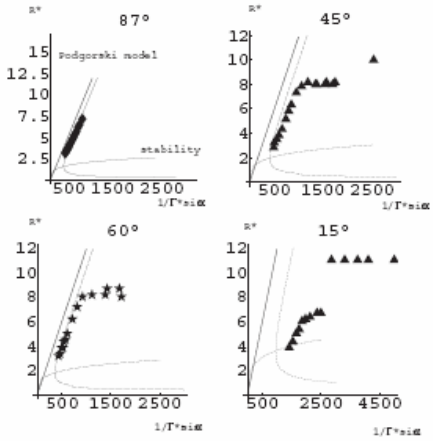

FIG. 2 – Theorie and experiments for a ($\eta = 18,5cP$) oil. $\Gamma^* = \frac{\Gamma}{U_c l_c}$ *and* $R^* = R/l_c$

In this work, we also investigate less viscous fluid where inertia plays an important role in the flow of both the film and the rim. This allow us to derive a new equilibrium shape and as for the viscous case we can introduce the capillary forces due to the radius of curvature to predict the loss of stability of the dry patch. A full model combining both inertial and Stokes limit is still on the progress

Références

[1] D. E. Hartley and W. Murgatroyd
Criteria for the break-up of thin liquid layers flowing isothermally over solid surfaces, Int. J. Heat Mass Transfer, 7,p 1003-1015,1964

[2] S. D. R. Wilson
The stability of a dry patch on a wetted wall, Int. J. Heat Mass Transfer, 17,p 1607-1615, 1974

[3] T. Podgorski, J-M Flesselles and L. Limat
Dry arches within flowing films, Physics of Fluids, 11, 4, 99

[4] S. K. Wilson and B. R. Duffy and S. H. Davis
On a slender dry patch in a liquid film draining under gravity down an inclined plane ,Euro. Jnl of Applied Mathematics, 12, p 233-252, 2001

21. A Finite Element Solution to the 3D Thermal Convection Problem

Christopher Smethurst
University of Manchester

By applying the Boussinesq approximation to the Navier-Stokes equations, which allows the fluid density to vary linearly with temperature in a gravitational field, and adding an equation for temperature, we get the Boussinesq equations. The Boussinesq equations model thermally-driven flow, i.e. flow in which convection occurs as a result of a buoyancy force between regions of fluid at different temperatures.
In general, numerical techniques are required to solve these equations. The finite element method is a general numerical procedure that can be applied to problems defined on a variety of domain shapes and that have complex boundary conditions, allowing more interesting and realistic problems to be solved.

Two case studies are carried out, one simulating the convection of liquid helium between two horizontal plates and another simulating the convection of liquid gallium in a cuboid cavity. Both cases are compared with experimental data.

22. Role of the channel geometry on the bubble pinch-off in flow-focusing devices

Wim van Hoeve
University of Twente

The role of the orifice geometry in the production of bubbles by flow focusing of a gas and a liquid in an orifice of rectangular cross-section is investigated. It is experimentally shown that the aspect ratio of the orifice dramatically influences the duration of bubble breakup, characterized by a slow linear 2D collapse, followed by a final fast 3D pinch-off. A stability analysis predicts that the 2D collapse is always stable, whereas the 3D pinch-off is always unstable. The ultimate stage of the pinch-off is recorded by high-speed imaging, yielding a scaling $w_m \sim\tau^{1/3}$ between the neck width w_m and the time τ before breakup, which indicates that breakup is driven solely by the inertia of both gas and liquid, and that it is not a capillary process. The presented study of the bubble breakup shows that elongated rectangular orifices favors high monodispersity, whereas the highest frequency of bubble production is achieved in square orifices.

23. An objective model of viscoelastic fluid: solvability of motion equations and attractors

D.A. Vorotnikov
Voronezh State University

We consider the initial-boundary value problem for the motion equations of an incompressible viscoelastic medium:

$$\frac{\partial u}{\partial t}+\sum_{i=1}^{n} u_i\frac{\partial u}{\partial x_i}+grad\ p=Div\ \sigma+f \tag{1}$$

$$\sigma+\lambda_1(\frac{\partial \sigma}{\partial t}+\sum_{i=1}^{n} u_i\frac{\partial \sigma}{\partial x_i}+\sigma W_\rho-W_\rho\sigma)$$

$$=2\eta(\mathcal{E}+\lambda_2(\frac{\partial \mathcal{E}}{\partial t}+\sum_{i=1}^{n} u_i\frac{\partial \mathcal{E}}{\partial x_i}+\mathcal{E}W_\rho-W_\rho\mathcal{E})) \tag{2}$$

$$div\ u=0 \tag{3}$$

$$u|_{t=0}=a,\ \sigma|_{t=0}=\sigma_0 \tag{4}$$

$$u|_{\mathbb{R}^n\setminus\Omega}=0 \tag{5}$$

Here u is an unknown velocity vector, p is an unknown pressure function, σ is an unknown tensor of shearing stresses (deviator of the stress tensor), f is the given body force (all of them depend on a point $x\in\mathbb{R}^n$ $(n\in\mathbb{N}, n>1)$ and on a moment of time t); Ω is a domain (subset of $\mathbb{R}^n$), where the fluid is moving; $\mathcal{E}$ is the strain velocity tensor: $\mathcal{E}_{ij}=\frac{1}{2}(\frac{\partial u_i}{\partial x_j}+\frac{\partial u_j}{\partial x_i})$, $\eta>0$ is the viscosity of the medium, λ_1 is the relaxation time, λ_2 is the retardation time, $0\le\lambda_2<\lambda_1$; a and σ_0 are given functions of x (vector and tensor, respectively), $W_\rho(t,x)=\int\limits_{\mathbb{R}^n} W(t,x-y)\rho(y)\,dy$ where W is the vorticity tensor: $W_{ij}=\frac{1}{2}(\frac{\partial u_i}{\partial x_j}-\frac{\partial u_j}{\partial x_i})$, and $\rho:\mathbb{R}^n\to\mathbb{R}$ is a smooth function with compact support, $\int\limits_{\mathbb{R}^n}\rho(y)\,dy=1$, $\rho(x)=\rho(y)$ for x and y with the same Euclidean norm. The gradient $grad$ and the divergence div are taken with respect to the variable x. The divergence $Div\ \sigma$ is the vector with the coordinates $(Div\ \sigma)_j=\sum\limits_{i=1}^{n}\frac{\partial \sigma_{ij}}{\partial x_i}$.

The constitutive law (2) is frame-indifferent (for the principle of material frame-indifference, see e.g. [1]), and may be considered as an n-dimensional generalization of the one-dimensional Maxwell ($\lambda_2=0$) and Jeffreys ($\lambda_2>0$) laws [2].

For $\Omega=\mathbb{R}^n$, we prove local in time existence of *strong* solutions to problem (1)-(4). For any open set $\Omega\subset\mathbb{R}^n$, $n=2,3$ and $\lambda_2>0$, we show existence of *weak* solutions to problem (1)-(5) (generalizing the result from [3]). We construct *trajectory* and *global attractors* (see the definitions in [4]) for these solutions.

The work was partially supported by RFBR and by BRHE Program of Ministry of Education and Science of Russia and CRDF.

References

[1] C. Truesdell. A first course in rational continuum mechanics, The John Hopkins University, Baltimore, 1972. [2] Reiner M. Rheology. In: Handbuch der Physik, S. Flugge (Ed.), Bd. VI, Springer, 1958. [3] D.A. Vorotnikov, V.G. Zvyagin, On the existence of weak solutions for the initial-boundary value problem in the Jeffreys model of motion of a viscoelastic medium, Abstr. Appl. Anal., 2004, V. 2004, no. 10, 815-829. [4] D.A. Vorotnikov, V.G. Zvyagin, Uniform attractors for non-autonomous motion equations of viscoelastic medium, J. Math. Anal. Appl., 2007, Volume 325, Issue 1, 438-458.

24. Numerical Simulation of Dynamic Stall using spectral/hp Methods

Medjroubi Wided, Pr.Dr. Joachim Peinke and Bernhard Stoevesandt
Oldenburg Universität

The need to reduce the costs of wind energy is increasing in the light of the increasing costs and the limited reserves of fossil energy, and the need of green sources of energy to limit the climate change, or global warming effect. The rentability of this source of energy and its implementation in large scales passes through the reduction of the costs of wind turbines. Since the blades cost constitutes a large part of the cost of the wind turbine (34 % for a medium-sized turbine 750Kw and 21% for a large turbine 1500 Kw) [1], there is a real need in producing more flexible, lighter and cheaper blades. To achieve this goal the accuracy and the reliability of the aerodynamic load prediction, produced by numerical simulation of the blades design, is of great importance. Additionally, the increasing size of the wind turbines triggers the need of a good prediction not only of the loads but also the effects of the rotation of the -constantly size increasing- blades on the rotor and the hole structure. The biggest challenge in the prediction of the loads on the wind turbines subject to unsteady flow conditions is the dynamic stall effect, which has destructive effects on the lift. It affects also the drag and moment coefficients. The dynamic stall involves the phenomenon of flow separation, which makes very challenging the accurate prediction of the physical coefficients as required by the industry of wind turbines manufacturing. Therefore the wind turbines dynamic stall must be well characterised and thoroughly understood, which is the main driving reason for this PhD project. Other motivations are also the use of the adaptive methods and moving grid techniques and the implementation of an appropriate model to simulate the unsteady and turbulent wind conditions. To achieve this goal we use the hp spectral code Nektar. This code was developed by the CRUNCH group at Brown University, under the direction of Prof. Dr Em. Karniadakis[2]. The Nektar code is a spectral elements Navier-Stokes solver with applications to compressible and incompressible fluids, magnetohydrodynamics (MHD), and in situations that involve moving boundaries using the Arbitrary Lagrangian Eulerian (ALE) formulation. The code is based on the spectral/hp method which is a combination of the flexibility of the finite elements (or finite volumes) methods and the high accuracy of the spectral methods[3]. My poster will include a short introduction to the topic of my PhD subject, the Nektar code features and some preliminary results at low Reynolds numbers.

[1] Hau, E. Wind Turbines; Fundamentales, Technologies, Application, Economics. Springer-Verlag Berlin. 2nd Edition. 2006.
[2] http://www.cfm.brown.edu/crunch/codes.html
[3] Karniadakis, G. E. and Sherwin, S. J. Spectral/HP Element Methods for CFD. Oxford University Press, Oxford, 1999.

25. Mixing by Steady Flows in Thermocapillary Driven Microdroplets

John Widloski
Georgia Institute of Technology

We consider microdroplets suspended at the free surface of a liquid substrate and mixed through chaotic advection induced by the thermocapillary effect. We illustrate that the mixing properties of the flow inside the droplet can vary dramatically as a function of the physical properties of the fluids and the imposed temperature profile. We show that to properly characterize the mixing requires the introduction of two different measures. The first measure determines the relative volumes of the domains of chaotic and regular streamlines. The second measure describes the time for homogenization inside the chaotic domain. Both measures are computed using pertubation theory in the limit

of weak temperature dependence of the surface tension coefficient at the free surface of the substrate.

26. Ripples on Fluid Ridges - now you see them, now you don't!

Johanna Ziegler
University of Bristol

When a volume of fluid runs down an inclined plate in a two-dimensional scenario - such that there are two solid/liquid/gas moving contact lines -, it tends to a steady state with a certain running speed Ca. We can solve the relevant equations numerically. For large volumes, we {f}ind a limiting speed Ca^* and a universal free surface shape consisting of a rounded front and a long trailing {f}ilm at the rear. There are also capillary ripples on the trailing film which help to match the two parts.
The relation between volume and running speed also shows an oscillation as it tends to Ca^* for large volumes, which is related to the physical capillary ripple and has the same wavelength. There is also a maximum speed Ca_{max} larger than Ca^* for a particular volume.
We observe a similar behaviour for a single contact line on a plate being drawn out of a liquid bath.
We can use a Landau-Levich argument to predict Ca^* in a certain limiting regime, and Ca_{max} for the one-contact line case obeys can be described asymptotically by an expression previously found by Eggers.